PROCEEDINGS OF THE YEREVAN STATE UNIVERSITY

Physical and Mathematical Sciences 2017, **51**(3), p. 269–274

P h y s i c s

INVESTIGATION OF LOCALIZED ELECTROMAGNETIC FIELD IN A SUBWAVELENGTH METALLIC SLIT

Sh. Kh. ARAKELYAN *

Chair of Microwave Radiophysics and Telecommunications YSU, Armenia

Electromagnetic field localization in a subwavelength metallic slit by a thermo-elastic optical indicator microscope (TEOIM) was investigated. As an indicator for the TEOIM system a slide glass with sizes of $20 \times 20 \times 0.5$ (mm) was used, on the surface of which an Al film of 20 *nm* thickness was vaporized using the vacuum evaporation technique, with various slit width $(10-50\ \mu m)$. Strongly localized electromagnetic field has been exited in the slits by 50 GHz generator and was visualized by a TEOIM. The waveguide properties of the system were characterized by COMSOL Multiphysics® additionally. The simulation results are in good agreement with the visualization data set.

***Keywords*:** subwavelength metallic slit, thermo-elasticity, visualization, field localization.

Introduction. Along with the development of electronics the miniaturization of waveguides become more important. Especially when the operation frequency is high enough and using of transmission lines and coaxial cables is not optional due to the high loss. Optical fibers are good enough for signal receiving application in optics, however they cannot be miniaturized below the diffraction order. In order to overcome this obstacle scientists and engineers have developed kinds of subwavelength waveguides, so called plasmonic waveguides [1,2], which also have been used in superfocusing applications [3]. A class of such waveguides are subwavelength slit waveguides consisting of two metallic plates and a dielectric media between them. Subwavelength slit waveguides and their properties were intensively investigated for some plasmonic and photonic applications [4–6], and they were widely used in various applications such as for the low-loss terahertz signal transmission [7], for the terahertz field enhancement [8], etc. Besides its waveguide properties the subwavelength slit structure also possesses a strong electric field (we will mention so the electric component of electromagnetic field) localization behavior in the metallic slit. This phenomenon may present a wide area of interest from the point of view of

* E-mail: shantaraqelyan@gmail.com

the electromagnetic field and material interaction. For such investigations, the ability to visualize electromagnetic field distributions is significant. As a such visualization technique, one can use the thermos-elastic optical indicator microscopy (TEOIM) system [9].

In this paper we realize an experimental investigation of the subwavelength slit waveguide, which has been excited by a 50 GHz oscillator. We use the TEOIM technique for the investigation of strongly localized electric field distribution. TEOIM system measures the mechanical stress distribution along the overall indicator surface and calculates the means of that mechanical stress by solving an inverse problem. Depending on the electromagnetic properties of the used indicator one can visualize both of electric or magnetic field distributions.

Materials and Methods. In this study we use the subwavelength slit waveguide as an indicator of TEOIM system. Additionally, in order to characterize the properties of the investigated waveguide we made COMSOL Multiphysics® simulations, the result of which were in good agreement with the experimental data.

The subwavelength slit waveguide investigation experimental setup is shown in Fig. 1. The setup represents itself a common TEOIM system only the indicator is replaced by the waveguide.

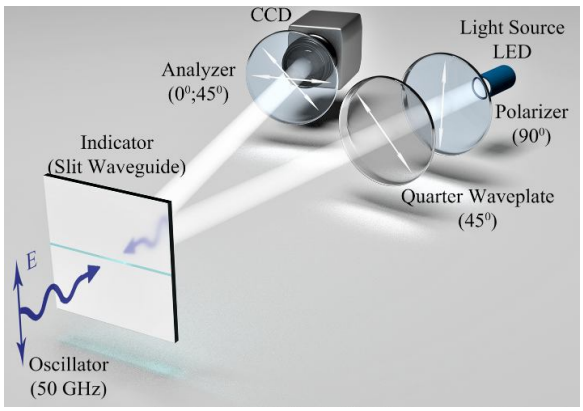

Fig. 1. The experimental setup for the electric field visualization.

Here the width of the metallic slit was varied in the range of 10–50 μm. Slit waveguides preparation was carried out by the vacuum evaporation technique, where we used special masks corresponding to the slit width. Deposition thickness was kept to be 20 nm, and we chose an aluminum as a metal for the deposition ($\sigma = 3.69 \cdot 10^7 S/m$). In the experimental setup we use a green light emitting diode ($\lambda = 530$ nm) as a light source, a polarizer and a quarter waveplate with the configuration shown in Fig. 1 to provide a circularly polarized incident light, the slit waveguide as an indicator, an analyzer, and a charge coupled device (CCD) camera. The slit waveguide was excited by the 50 GHz oscillator, the electric field polarization of which is perpendicular to the slit.

When the oscillator radiation is turned on, the waveguide couples the electromagnetic field energy and a strongly localized electric field appears in the

slit. Due to that strong electric field localization, the indicator heats up and changes the incident circularly polarization state to elliptical during the reflection due to the photo-elastic effect. Thus, the reflected light becomes elliptically polarized and by choosing the analyzer orientation to be 0 or 45° one can obtain two linear birefringent distribution images related to normal and shear components of the mechanical stress tensor of the indicator.

The final electric field distribution is calculated by solving the inverse problem of the mechanical stress formation. More detailed information about the TEOIM measurement principle and image processing procedure are described in [9]. Note that the experimental setup has been adjusted on the optical table and all changes in it has been done remotely. All measurements and image processing procedure have been implemented by a custom program made in the LabVIEW interface.

Results and Discussion. Fig. 2 shows the TEOIM visualization results corresponding to the 10 (a) and 50 μm (b) of the slit width. One can see the visualized intensity is drastically decreased when the slit width increases. Note that the most intense area of the indicator corresponds to the oscillator location.

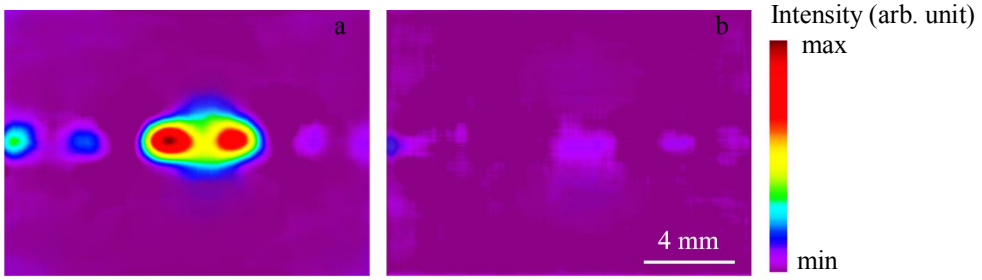

Fig. 2. The TEOIM visualization results: (a) 10 μm and (b) 50 μm of the slit width.

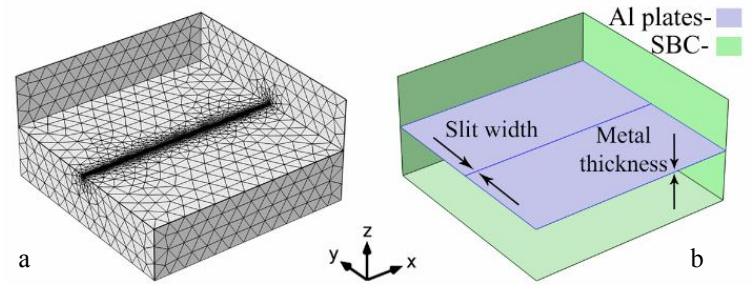

Fig. 3. COMSOL Multiphysics simulation: a) the meshed geometry of the model; b) the indication of "Scattering Boundary Conditions" and Aluminum plates.

In this experiment the thickness of the aluminum was 20 nm and the oscillator operation frequency was 50 GHz. In such situation the relation between the metallic plates and skin-depth ($\delta = 366.7$ nm at 50 GHz) consists $1:18$. One can see from

Fig. 2, that during the propagation the most part of the energy is absorbed. This phenomenon is conditioned by the sub-skin-depth thickness of the metallic plates, since in this case the electrical conductivity becomes lower [10].

In order to compare the simulated and experimental data, we built COMSOL Multiphysics® simulation. Fig. 3 shows the simulation model. Here we used "Transition Boundary Condition" in a modeling of the metallic plates of the waveguide. The width of the slit and the thickness of metallic plates in the simulated model have been varied in the range of 20–100 *nm* and 10–50 μm respectively.

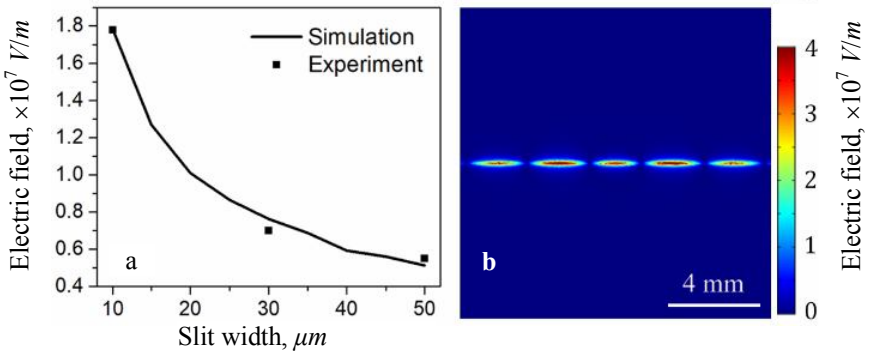

Fig. 4. Simulation results: a) the electric field intensity dependence on the slit width; b) the field distribution for the 10 μm slit.

Fig. 4 shows the results of the simulation, where the thickness of the aluminum is kept to be 20 *nm*. Fig. 4, a presents the dependence of the localized electric field on the slit width. One can see that values corresponding to the experimental visualizations are in good agreement with the simulated data. Fig. 4, b corresponds to the case when the slit width is 10 μm (same as in Fig. 2, a). Note that the differences between the visualized (Fig. 2, a) and the simulated (Fig. 4, b) intensity distributions can be explained, if one takes into account the specification of the TEOIM visualization technique, i.e. the heat transfer overall the indicator surface. When the strong electric field heats up the indicator a part of the heat is diffused along the that the differences between the visualized (Fig. 2, a) and the simulated (Fig. 4, b) intensity distributions can be explained, if one takes into account the specification of the TEOIM perpendicular direction of the slit. Thus, the shape of the visualized intensity becomes broader compared with the simulation case.

In order to obtain a detailed information about the electric field localization in the subwavelength metallic slit, we performed two-dimensional parametric sweep of the slit width and metal thickness. The result is depicted in Fig. 5. One can see that the electric field localization possesses non-resonant behavior in the investigated range of the slot width and metal thickness. The electric field intensity monotonically decreases parallel to the increasing of the slit width and decreasing of the metal thickness.

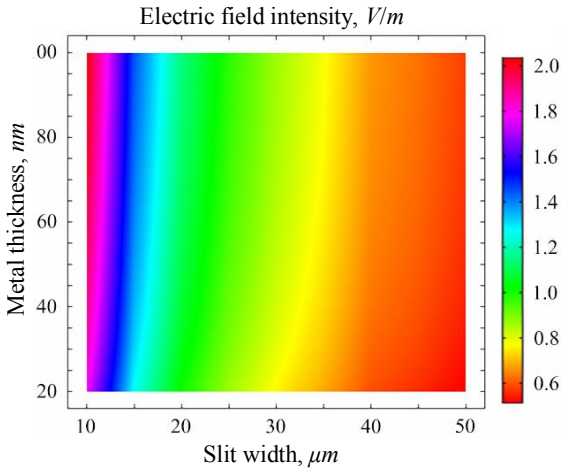

Fig. 5. The averaged electric field dependence on the slit width and metal thickness.

This result may help to find necessary parameters of the subwavelength slit waveguide for the desired strength of the electric field localization. It also may be helpful to characterize the electrical conductivity of sub-skin-depth metallic layers.

Conclusion. We succeeded in visualizing the electric field intensity in the subwavelength metallic slit by the TEOIM technique. We find out that the electric field localization possesses non-resonant behavior in the investigated range of the waveguide parameters. It has been experimentally shown that even in the case of 1 : 18 relation of the metal thickness and skin depth, the strongly localized electric field appears in the metallic slit.

Received 10.07.2017

REFERENCES

1. **Pile D.F.P., Gramotnev D.K.** Plasmonic Subwavelength Waveguides: Next to Zero Losses at Sharp Bends. // Opt. Lett., 2005, v. 30, № 10, p. 1186.
2. **Bozhevolnyi S.I., Volkov V.S., Devaux E., Laluet J.-Y., Ebbesen T.W.** Channel Plasmon Subwavelength Waveguide Components Including Interferometers and Ring Resonators. // Nature, 2006, v. 440, № 7083, p. 508–511.
3. **Nerkararyan Kh.V.** Superfocusing of a Surface Polariton in a Wedge-Like Structure. // Phys. Lett. A, 1997, v. 237, № 1–2, p. 103–105.

4. **Pors A., Nerkararyan Kh.V., Sahakyan K., Bozhevolnyi S.I.** Enhanced Non-resonant Light Transmission Through Subwavelength Slits in Metal. // Opt. Lett., 2016, v. 41, № 2, p. 242.
5. **Veronis G., Fan S.** Modes of Subwavelength Plasmonic Slot Waveguides. // J. Light. Technol., 2007, v. 25, № 9, p. 2511–2521.
6. **Kong F., Li K., Huang H., Wu B.-I., Kong J.A.** Analysis of the Surface Magnetoplasmon Modes in the Semiconductor Slit Waveguide at Terahertz Frequencies. // Prog. Electromagn. Res., 2008, v. 82, p. 257–270.
7. **Wächter M., Nagel M., Kurz H.** Metallic Slit Waveguide for Dispersion-Free Low-Loss Terahertz Signal Transmission. // Appl. Phys. Lett., 2007, v. 90, № 6, p. 061111.
8. **Seo M.A.** et al. Terahertz Field Enhancement by a Metallic Nano Slit Operating Beyond the Skin-Depth Limit. // Nat. Photonics, 2009, v. 3, № 3, p. 152–156.
9. **Lee H., Arakelyan S., Friedman B., Lee K.** Temperature and Microwave Near Field Imaging by Thermo-Elastic Optical Indicator Microscopy. // Sci. Rep., 2016, v. 6, № 1, p. 39696.
10. **Bosman H., Lau Y.Y., Gilgenbach R.M.** Microwave Absorption on a Thin Film. // Appl. Phys. Lett., 2003, v. 82, № 9, p. 1353.